Modeling traffic forecasts with probability in DWDM optical networks

Stanisław Kozdrowski[1,2][0000−0001−6647−5189],
Piotr Sliwka[3,4][0000−0001−6226−9580], and
Sławomir Sujecki[5,6][0000−0003−4588−6741]

[1] Department of Computer Science, Faculty of Electronics,
Warsaw University of Technology,
Nowowiejska 15/19, 00-665 Warsaw, Poland
[2] s.kozdrowski@elka.pw.edu.pl
[3] Department of Computer Science, Cardinal Wyszynski University
Woycickiego 1/3, 01-938, Warsaw, Poland
[4] p.sliwka@uksw.edu.pl
[5] Telecommunications and Teleinformatics Department,
Wroclaw University of Science and Technology,
Wyb. Wyspianskiego 27, 50-370 Wroclaw, Poland
[6] Slawomir.Sujecki@pwr.edu.pl

Abstract. Dense wavelength division multiplexed networks enable operators to use more efficiently the bandwidth offered by a single fiber pair and thus make significant savings, both in operational and capital expenditures. In this study traffic demands pattern forecasts (with probability) in subsequent years are calculated using statistical methods. Subject to results of statistical analysis numerical methods are used to calculate traffic intensity in edges of a dense wavelength division multiplexed network both in terms of the number of channels allocated and the total throughput expressed in gigabits per second. For the calculation of traffic intensity a model based on mixed integer programming is proposed, which includes a detailed description of optical network resources. The study is performed for a practically relevant network within selected scenarios determined by realistic traffic demand sets.

Keywords: DWDM System Design · Optical Network Optimization · CDC-F technology · Optical Node Model · Network Congestion · Mixed Integer Programming (MIP) · Forecasting with Probability · Time Series

1 Introduction

Optical networks based on Dense Wavelength Division Multiplexing (DWDM) technology form the backbone of today's telecommunications industry. To meet ever increasing traffic demands DWDM systems undergo constant development aimed at increasing the network capacity. For this purpose new concepts within DWDM network paradigm are proposed and studied, e.g. Ultra Wideband DWDM (UW-DWDM) systems or Space Division Multiplexing (SDM) systems.

ICCS Camera Ready Version 2021
To cite this paper please use the final published version:
DOI: 10.1007/978-3-030-77970-2_28

From the network operator point of view, the ever increasing demand for high speed data services translates into the need to continually upgrade the networks to increase the data transmission rate per optical fiber. In currently deployed optical networks, which are based on single core fibers, the data transmission rate can be increased by using either a larger per-channel bit rate or by increasing the number of available channels [9].

Existing fiber optic networks that operate in C-band (1530 nm to 1565 nm) typically support up to 96 channels of 50 GHz bandwidth. The selection of the C-band for optical long-haul communications is low light attenuation in silica glass fiber and availability of high quality, low cost erbium ion doped fiber amplifiers (EDFAs). Additional capacity in C-band DWDM systems can be gained by using flexible grid, which enables provisioning flexible size DWDM channels with bandwidth as small as 12.5 GHz and the carrier wavelength step of 6.25 GHz. This allows for a more effective use of the available bandwidth within the C-band by reducing the guard bands. A significant proportion of operational expenditure for such networks is the cost of fiber lease which is usually quoted per fiber length unit [1].

During the last decade attention of the telecommunication community has been concentrated on Routing and Wavelength Assignment (RWA) and Routing and Spectrum Allocation (RSA) problems in static [6, 7, 3, 8] and dynamic [17, 18, 4] environment. This study concentrates on the analysis of DWDM networks, which not only pertains to the traffic present in the network but also allows for gaining insight into the future network development needed to meet the predicted demands matrix evolution.

In this article a statistical analysis of network traffic is performed based on the empirical data and used to calculate traffic forecasts. The application of statistical methods leads to calculation of the elements of the traffic demands matrix and their forecasts for the coming years. Subject to calculated values of the traffic demands matrix elements numerical methods are applied to calculate traffic intensity in the edges of a dense wavelength division multiplexed network both in terms of the number of channels allocated and the total throughput expressed in gigabits per second. For the calculation of traffic intensity a model based on integer programming is proposed, which includes a detailed description of optical network resources. Integer programming performs network cost optimisation subject to given data on traffic demand pattern predictions for subsequent time periods that was obtained using the aforementioned statistical methods. Network topology used in the simulations is realistic and representative for optical networks, and stems from [10].

The rest of the paper is organized as follows. In the second section, the mathematical background relevant to the applied optimizing procedures and statistical analysis is considered. In the third section, the usefulness of the proposed theoretical model is discussed in the context of the empirical data and is followed by a concise summary given in the last section.

ICCS Camera Ready Version 2021
To cite this paper please use the final published version:
DOI: 10.1007/978-3-030-77970-2_28

2 Problem formulation

As the case study a Polish network was selected (Figure 1). Empirical data on the actual demand for transmission rates in the network between individual cities is not available. Real data on the volume of demand and the resulting transmission rates is usually proprietary to companies providing telecommunication services. Due to these constraints, the demand bandwidth for the access in the network nodes were determined assuming that the maximum demand for the bandwidth is a combination of demographic[7](the percentage share of people aged over 14 in the cities of Poland considered) and the percentage of households with broadband access in 6 Polish macro-regions and separately for the Mazowieckie Voivodeship[8] in the period 2010-2019. Based on the above empirical data, optimal demands were determined, as well as their forecasts for 2020-2024.

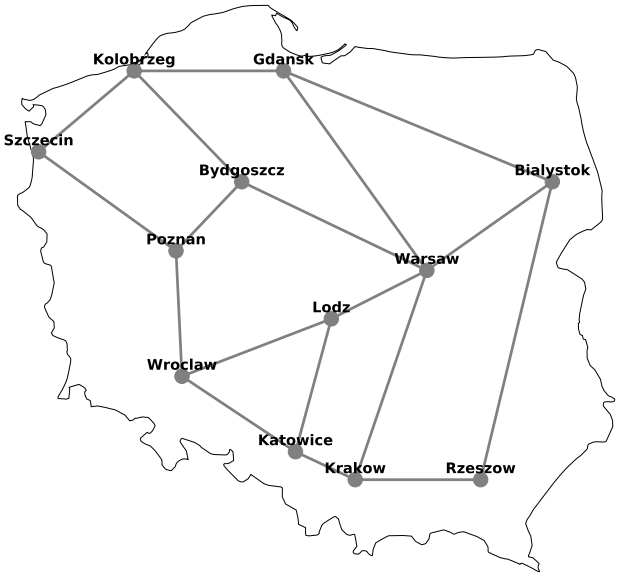

Fig. 1: Schematic diagram of Polish national transmission optical network.

It is noted that the selection of the forecasting method depends on the phenomenon that one wants to forecast. The construction of long-term forecasts and the related methodology assumes that the time series of empirical data on

[7] based on Statistics Poland data
[8] based on Eurostat

ICCS Camera Ready Version 2021
To cite this paper please use the final published version:
DOI: 10.1007/978-3-030-77970-2_28

the basis of which these forecasts are built meet at least stationary condition in wide-sense (the 1st moment and autocovariance do not depend on time t and the 2nd moment is finite for all t). Otherwise, short-term forecasts are made (for several periods ahead more about the use of short-term forecasting methods in [13–16]). Due to the very short time series of observations y_t available in this study, basic forecasting tools were used and short-term forecasts were made. Therefore, a linear or logarithmic trend depending on the nature of the empirical data was applied to model demand and objective function values. For the case studied the obtained estimates of the trend function parameters, from a statistical point of view, are significant (p-value for each estimated parameter of the corresponding trend model is < 0.05, where 0.05 - a significance level) and the coefficient of determination R^2 is greater than 85%, reaching 98.5% in some cases, which means that the model is very well fit to empirical data.

One of the goals of this article is to determine the point forecast and the interval forecast with the appropriate probability. The $N(\mu, \sigma)$ distribution, bootstrap or resampling methods are usually used to determine the limits of the forecast confidence interval. In our case, due to the very small number of observations, the above methods cannot be used (the distribution of the e_t is not characterized by $N(\mu, \sigma)$). Therefore, a point forecast was determined for each edge, and then, taking into account the distribution of e_t residuals, as well as the naive forecast of e_t, the minimum and maximum forecast values were determined for this edge with an appropriate probability of its implementation (assumption: invariance of distribution of residuals e_t). For example, in the case of the Wroclaw-Lodz edge, the histogram of residuals e_{WrLo} for 3 classes gives the following distribution of values: $-0.0059, -0.0022, 0.0014, 0.0051$ with the respective probabilities: 0.2, 0.5 and 0.3 for the intervals: $\{-0.0059, -0.0022\}$, $\{-0.0022, 0.0014\}$, $\{0.0014, 0.0051\}$, where $e_{MIN_{WrLo}} = -0.0059$ is its left limit, and $e_{MAX_{WrLo}} = 0.0051$ right limit. Based on the predicted theoretical value of $\hat{y}_{WrLo_t}$ from the model and the dependence $y_t = e_t + \hat{y}_t$, the "real" value can be determined. The coefficients of the lower and upper matrix of the predicted values of $\hat{y}_t$ with the appropriate probability were determined in a similar way.

Knowing: a) the distribution of the residuals e_t over the period 2010 – 2019, b) the probability of meeting the maximum and minimum demand (in the figures as Max and Min, respectively) during the period 2010 – 2019 and c) point forecasts for 2020 – 2024, the thresholds have been set for the forecast between 2020 and 2024 to be realised with appropriate probability. Due to the problem of network congestion, which is taken into account here in particular, the main focus is on the top end of the $\hat{y}_{max}$ range, i.e. the maximum value of demand realised and probability of their occurrence.

Finally, one calculates the demand matrix elements, which provide the values of traffic flow between selected nodes expressed in Gbps. An example of a matrix of coefficients based on empirical data described in Section 2 only for level 0, and the corresponding demand matrix in 2020 for level 0 as well as additionally for the Min and Max levels with the probability of their occurrence (in parentheses) for the network in Fig. 1 are presented in tables 1-4 respectively.

ICCS Camera Ready Version 2021
To cite this paper please use the final published version:
DOI: 10.1007/978-3-030-77970-2_28

Table 1: An example of coefficient matrix: forecast, 2020, level 0.

	2	3	4	5	6	7	8	9	10	11	12
1	0.109	0.0758	0.1007	0.1624	0.1007	0.1514	0.1307	0.087	0.1144	0.3012	0.1457
2		0.061	0.0859	0.1476	0.0859	0.1366	0.1159	0.0722	0.0996	0.2864	0.1309
3			0.0527	0.1145	0.0528	0.1035	0.0827	0.039	0.0665	0.2532	0.0977
4				0.1393	0.0776	0.1283	0.1076	0.0639	0.0914	0.2781	0.1226
5					0.1393	0.19	0.1693	0.1256	0.1531	0.3398	0.1843
6						0.1283	0.1076	0.0639	0.0914	0.2781	0.1226
7							0.1583	0.1146	0.1421	0.3288	0.1733
8								0.0939	0.1213	0.3081	0.1526
9									0.0776	0.2644	0.1089
10										0.2919	0.1363
11											0.3231

Table 2: An example of demands matrix: forecast, 2020, level Min (probability).

	2	3	4	5	6	7	8	9	10	11	12
1	1293 (0.3)	898 (0.2)	1190 (0.2)	1917 (0.2)	1201 (0.3)	1799 (0.4)	1543 (0.2)	1040 (0.5)	1353 (0.2)	3585 (0.3)	1728 (0.1)
2		724 (0.3)	1016 (0.2)	1745 (0.2)	1019 (0.3)	1619 (0.4)	1369 (0.2)	859 (0.4)	1179 (0.2)	3412 (0.4)	1548 (0.2)
3			624 (0.2)	1354 (0.3)	619 (0.2)	1223 (0.3)	974 (0.2)	459 (0.2)	784 (0.2)	3021 (0.4)	1145 (0.2)
4				1652 (0.3)	913 (0.3)	1518 (0.5)	1269 (0.2)	753 (0.2)	1079 (0.2)	3318 (0.4)	1436 (0.2)
5					1651 (0.4)	2257 (0.4)	1997 (0.2)	1492 (0.4)	1808 (0.2)	4048 (0.4)	2179 (0.3)
6						1513 (0.3)	1271 (0.2)	752 (0.4)	1077 (0.2)	3313 (0.4)	1440 (0.2)
7							1872 (0.3)	1353 (0.3)	1680 (0.3)	3918 (0.4)	2053 (0.2)
8								1110 (0.2)	1430 (0.2)	3664 (0.2)	1814 (0.3)
9									917 (0.2)	3153 (0.4)	1275 (0.1)
10										3475 (0.3)	1616 (0.3)
11											3853 (0.3)

Table 3: An example of demands matrix: forecast, 2020, level 0.

	2	3	4	5	6	7	8	9	10	11	12
1	1307	910	1208	1949	1208	1817	1568	1044	1373	3614	1748
2		732	1030	1771	1031	1639	1390	866	1196	3437	1570
3			633	1374	633	1242	993	468	798	3039	1173
4				1672	931	1540	1291	767	1096	3337	1471
5					1672	2281	2032	1507	1837	4078	2212
6						1540	1291	767	1097	3337	1471
7							1900	1375	1705	3946	2080
8								1126	1456	3697	1831
9									932	3173	1306
10										3502	1636
11											3877

Once the elements of the demand matrix are determined the data traffic intensity in edges of the analysed network are calculated using Mixed Integer Programming (MIP). For this purpose the following sets are defined:

ICCS Camera Ready Version 2021
To cite this paper please use the final published version:
DOI: 10.1007/978-3-030-77970-2_28

Table 4: An example of demands matrix: forecast, 2020, level Max (probability).

	2	3	4	5	6	7	8	9	10	11	12
1	1321 (0.2)	918 (0.3)	1220 (0.3)	1972 (0.2)	1221 (0.2)	1833 (0.3)	1577 (0.4)	1056 (0.2)	1383 (0.4)	3636 (0.3)	1760 (0.3)
2		740 (0.2)	1042 (0.3)	1798 (0.2)	1040 (0.3)	1654 (0.3)	1400 (0.4)	875 (0.3)	1205 (0.4)	3461 (0.3)	1580 (0.4)
3			646 (0.2)	1402 (0.2)	634 (0.6)	1257 (0.4)	997 (0.5)	469 (0.6)	801 (0.5)	3066 (0.3)	1173 (0.6)
4				1716 (0.2)	943 (0.4)	1569 (0.4)	1302 (0.4)	780 (0.4)	1109 (0.2)	3379 (0.2)	1469 (0.6)
5					1704 (0.2)	2329 (0.2)	2057 (0.2)	1540 (0.2)	1864 (0.2)	4135 (0.2)	2230 (0.4)
6						1554 (0.4)	1296 (0.5)	773 (0.5)	1100 (0.5)	3364 (0.4)	1478 (0.5)
7							1915 (0.4)	1391 (0.4)	1720 (0.4)	3990 (0.4)	2097 (0.3)
8								1131 (0.4)	1462 (0.5)	3721 (0.3)	1846 (0.4)
9									935 (0.4)	3201 (0.4)	1310 (0.6)
10										3527 (0.3)	1646 (0.4)
11											3897 (0.3)

$\mathcal{N}$ set of all nodes
$\mathcal{T}$ set of transponders
$\mathcal{S}$ set of frequency slices
$\mathcal{E}$ set of edges
$\mathcal{P}_{(n,n')}$ set of paths between nodes $n, n' \in \mathcal{N}$; $p \subseteq \mathcal{E}$
$\mathcal{B}$ set of bands
$\mathcal{S}_b$ set of frequency slices used by band $b \in \mathcal{B}$; $\mathcal{S}_b \subseteq \mathcal{S}$; $\bigcup_{b \in \mathcal{B}} \mathcal{S}_b = \mathcal{S}$
$\mathcal{S}_t$ set of frequency slices that can be used as starting slices for transponder $t \in \mathcal{T}$; $\mathcal{S}_t \subseteq \mathcal{S}$

The following objective cost function is optimized using a MIP algorithm subject to the listed below constraints:

$$\min \left\{ \sum_{b \in \mathcal{B}} \left\{ \xi_1(b) \sum_{e \in \mathcal{E}} y_{be} + \sum_{t \in \mathcal{T}} \xi_2(t,b) \sum_{n,n' \in \mathcal{N}} \sum_{p \in \mathcal{P}_{(n,n')}} \sum_{s \in \mathcal{S}_t} x_{tnn'ps} \right\} \right\} \tag{1}$$

where, $\xi_1(b)$ is a cost of using band b at a single edge, y_{be} is a binary variable, equals 1 if band b is used on edge e and 0 otherwise, $\xi_2(t,b)$ is a cost of using a pair of transponders t in band b and $x_{tnn'ps}$ is a binary variable that equals 1 if transponders t are installed between node n and node n', routed on path p, and starting on frequency slice $s \in \mathcal{S}_t$ and 0 otherwise.

In the model the following three constraints have been included:

$$\sum_{t \in \mathcal{T}} \sum_{p \in \mathcal{P}_{(n,n')}} \sum_{s \in \mathcal{S}_t} v(t) x_{tnn'ps} \geq d(n,n') \quad \forall n, n' \in \mathcal{N} \tag{2}$$

ICCS Camera Ready Version 2021
To cite this paper please use the final published version:
DOI: 10.1007/978-3-030-77970-2_28

where, $v(t)$ is a bitrate provided by transponder t and $d(n, n')$ is a bitrate demanded from node n to node n'.

$$\begin{aligned} x_{tnn'ps} h\nu(b) c(t) \Delta(t) \sum_{e \in \mathcal{E}} w(n, n', p, e) \cdot \\ \cdot \left(f(e)(e^{\frac{\lambda(s) l(e)}{1+f(e)}} + V - 2) + (e^{\frac{\lambda(s) l(e)}{1+f(e)}} + W - 2) \right) \leq P_0 \\ \forall t \in \mathcal{T},\ \forall n, n' \in \mathcal{N},\ \forall p \in \mathcal{P}_{(n,n')},\ \forall b \in \mathcal{B},\ \forall s \in \mathcal{S}_b \end{aligned} \tag{3}$$

where, h is the Planck constant equal to $6.62607004 \cdot 10^{-34} m^2 kg/s$, $\nu(b)$ is a frequency of band b, $c(t)$ is an Optical Signal to Noise Ratio (OSNR) of transponder t, which has been calculated using the standard formula, c.f. [2, 12, 11, 5]. $\Delta(t)$ is the bandwidth used by a transponder t, $f(e)$ is a number of In-Line Amplifiers (ILAs) evenly distributed over edge e to re-amplify the signal in order to prevent OSNR from dropping to a very small value, $\lambda(s)$ is a loss per km using slice s, $l(e)$ is a length of edge e, V is the gain of ILA, W is the gain of fibre amplifier that compensates the nodal loss while the transmitter output power for a single WDM channel is assumed to equal to 1 mW and is represented by P_0. Finally, a constraint is added for avoiding duplicate allocation of the same wavelength in an edge:

$$\begin{aligned} \sum_{t \in \mathcal{T}} \sum_{n,n' \in \mathcal{N}} \sum_{p \in \mathcal{P}_{(n,n')}} \sum_{s \in \mathcal{S}_t} w(n, n', p, e) u(t, s, s') x_{tnn'ps} \leq y_{be} \\ \forall e \in \mathcal{E},\ \forall b \in \mathcal{B},\ \forall s' \in \mathcal{S}_b \end{aligned} \tag{4}$$

where, $w(n, n', p, e)$ is a binary constant that equals 1 if a path p between nodes n and n' uses edges e and 0 otherwise, $u(t, s, s')$ is a binary constant that equals 1 if transponder t using bandwidth starting at frequency slice s also uses frequency slice s' and 0 otherwise.

The subject of minimization is the cost of installed amplifiers and transponders in (1). Constraints (2) ensure that all demands are satisfied. Constraints (3) ensure that all installed transponders are routed in such a way that their power budgets are not exceeded. Notice that these constraints can be precalculated and reduced to $x_{tnn'ps} = 0$ for some combinations of indices and removed for other combinations. Finally, (4) ensure that using a band results in installing appropriate amplifiers. Notice that these constraints also ensure that each frequency slice at each edge is not used more than once. It is noted that the constraints included do not allow for considering nonlinear interactions and resulting signal impairments.

Once the MIP problem is solved the number of the allocated channels and total throughput for each network edge is determined, which is the objective of this study. Section 3 provides illustrative examples for the network studied.

ICCS Camera Ready Version 2021
To cite this paper please use the final published version:
DOI: 10.1007/978-3-030-77970-2_28

3 Results and Discussion

This section presents the results of computational experiments obtained by applying algorithms described in section 2 to empirical data collected over the time span ranging from year 2010 until 2019. The objective of the simulations is first to forecast the elements of the demand matrix for the next years (2020 – 2024) and to calculate traffic intensity in the edges of a dense wavelength division multiplexed network both in terms of the number of channels allocated and the total throughput expressed in gigabits per second. Once the results are obtained the identification of the bottlenecks of the network studied is performed with intent to predict the time at which the capacity of a given network edge will achieve its limit and also to find network edges, which do not carry traffic.

Computational results were obtained for Polish national network, which topology is depicted in Fig. 1. The topology of the network was taken from [10]. The analyzed network consists of 12 nodes, 18 links and 66 traffic demands. The traffic demands (demand matrix elements) were calculated using statistical methods described in section 2.

3.1 Simulation parameters

Table 5a describes in detail the sets used by the optimisation procedures while Table 5b lists modelling parameters used for performing computations. Note, that the constants given in the first column of Table 5b are defined in section 2.

Table 5: Sets and modelling parameters description.

Set	Set settings
$\mathcal{N}$	12
$\mathcal{E}$	18
$\mathcal{S}$	96 slots (opt. ch.)
$\mathcal{B}$	1 band
$\mathcal{T}$	3 transponders
$\mathcal{S}_b$	$\mathcal{S}_1 = \{1 \dots 96\}$
$\mathcal{S}_t$	$\mathcal{S}_1 = \{1 \dots 95\}$ $\mathcal{S}_2 = \{1 \dots 95\}$ $\mathcal{S}_3 = \{1 \dots 95\}$

(a) Set settings.

Constant	Constant settings
bitrate [Gbps]	$v(1) = 100$, $v(2) = 200$, $v(3) = 400$
OSNR[dB]	$c(1) = 12$, $c(2) = 15$, $c(3) = 22$
d(n,n')[Gbps]	an example in Tables 2 – 4
$\xi_2(t, b)$	$\xi_2(1, 1) = 5$, $\xi_2(2, 1) = 7$, $\xi_2(3, 1) = 9$
$\Delta(t)$[GHz]	$\Delta(1) = \Delta(2) = \Delta(3) = 50$
$\nu(b)$[THz]	$\nu(1) = 193.8$
$\lambda(s)$[dB/km]	$\lambda(s) = 0.046$
W, V[dB]	15
P_0[W]	10^{-3}

(b) Constant settings.

The calculations were carried out using a linear solver engine of CPLEX 12.8.0.0 on a 2.1 GHz Xeon E7-4830 v.3 processor with 256 GB RAM running under Linux Debian operating system. The average calculation time for one particular result was approximately equal to 1800 s.

ICCS Camera Ready Version 2021
To cite this paper please use the final published version:
DOI: 10.1007/978-3-030-77970-2_28

3.2 Results

Figure 2 presents the percentage of allocated channels in a network edge calculated for the empirical data, i.e. up until year 2019 whilst Figs 3 – 5 show analogous results calculated for the statistically estimated forecasts, i.e. years 2020 – 2024. The results shown in Figs 2 – 5 are presented in a form of network maps, which helps fast identification of network edges, which are either unused or used to the full capacity.

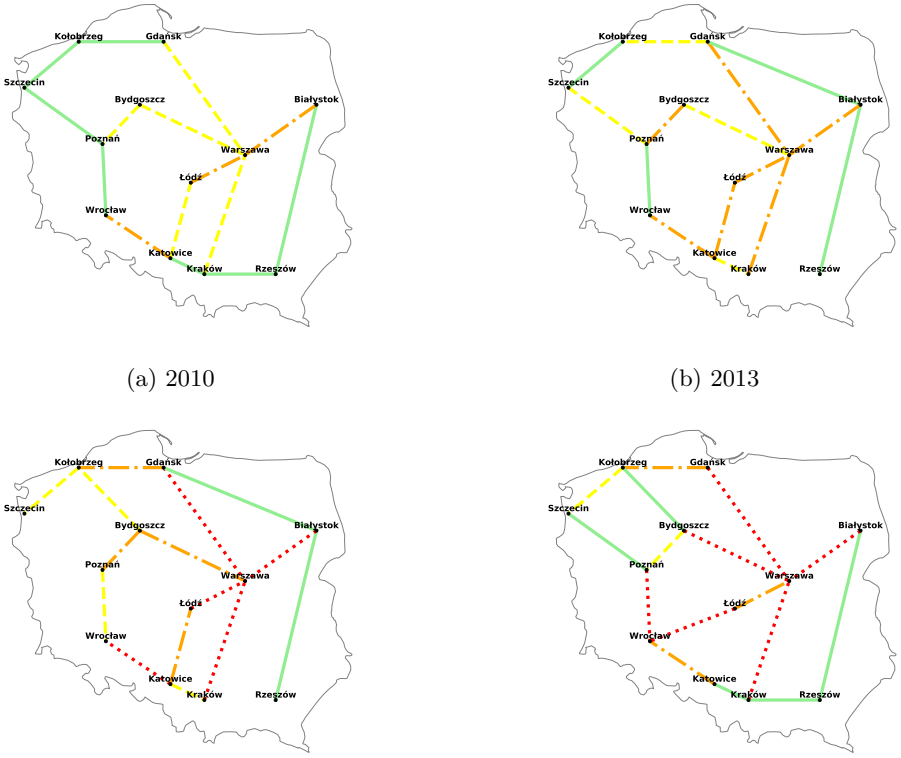

(a) 2010

(b) 2013

(c) 2016

(d) 2019

Fig. 2: The percentage of bandwidth used for all edges: 0%-70% - solid line, 71%-90% - dashed line, 91%-99% - dotted-dashed line and 100% - dotted line; empirical data, 2010-2019.

Figures 6 – 7 show the values for the number of the allocated channels and total throughput for given years calculated for the empirical data (Figure 6, years 2010 – 2019) and forecasts (Figure 7, years 2020 – 2024). The values of the allocated channels and total throughput were obtained by summing over all

ICCS Camera Ready Version 2021
To cite this paper please use the final published version:
DOI: 10.1007/978-3-030-77970-2_28

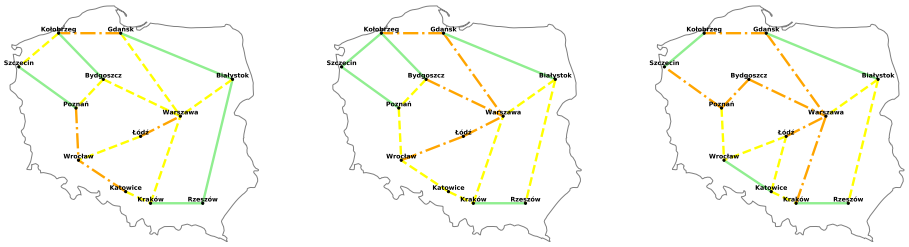

(a) Min (b) 0 (c) Max

Fig. 3: The percentage of bandwidth used for all edges: 0%-70% - solid line, 71%-90% - dashed line, 91%-99% - dotted-dashed line and 100% - dotted line in levels: Min, 0, Max; forecast, 2020.

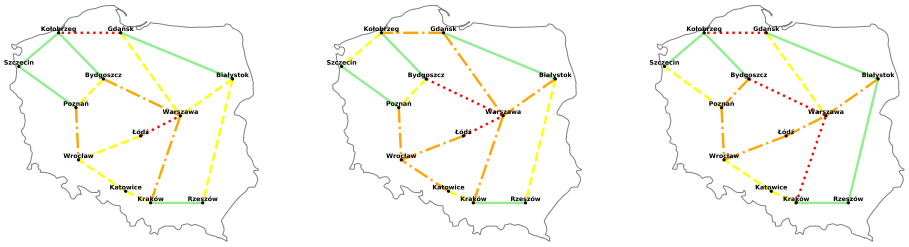

(a) Min (b) 0 (c) Max

Fig. 4: The percentage of bandwidth used for all edges: 0%-70% - solid line, 71%-90% - dashed line, 91%-99% - dotted-dashed line and 100% - dotted line in levels: Min, 0, Max; forecast, 2022.

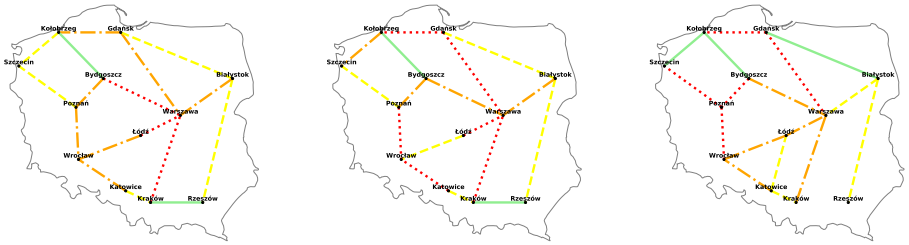

(a) Min (b) 0 (c) Max

Fig. 5: The percentage of bandwidth used for all edges: 0%-70% - solid line, 71%-90% - dashed line, 91%-99% - dotted-dashed line and 100% - dotted line in levels: Min, 0, Max; forecast, 2024.

ICCS Camera Ready Version 2021
To cite this paper please use the final published version:
DOI: 10.1007/978-3-030-77970-2_28

network edges. Based on the results presented in Figs 2 - 5 one can make several observations that are potentially relevant to a network management team:

– some edges are not used at all, e.g. the edge Bialystok - Gdansk, Lodz - Wroclaw and Poznan - Bydgoszcz (Figure 2a), or Gdansk - Bialystok and Bydgoszcz - Poznan (Figure 2d),
– for the empirical data (Figure 2), up to 16 edges were used between 2010 and 2019, out of the total of 18 possible edges. For the forecasts (Figure 3 – 5b) 17 edges were used out of 18 possible,
– in the last year of empirical data (Figure 2d), even though as many as 6 edges reached saturation, still 2 edges were not used at all. The utilisation of further edges takes place in the year 2020 (Figure 3b), but instead some other edges are relieved,
– in the initial forecast period (2020), the network still large proportion of not allocated resources (Figure 3b). In contrast, in 2022 – 2024 increasingly many edges reach saturation (Figure 4b – 5b).

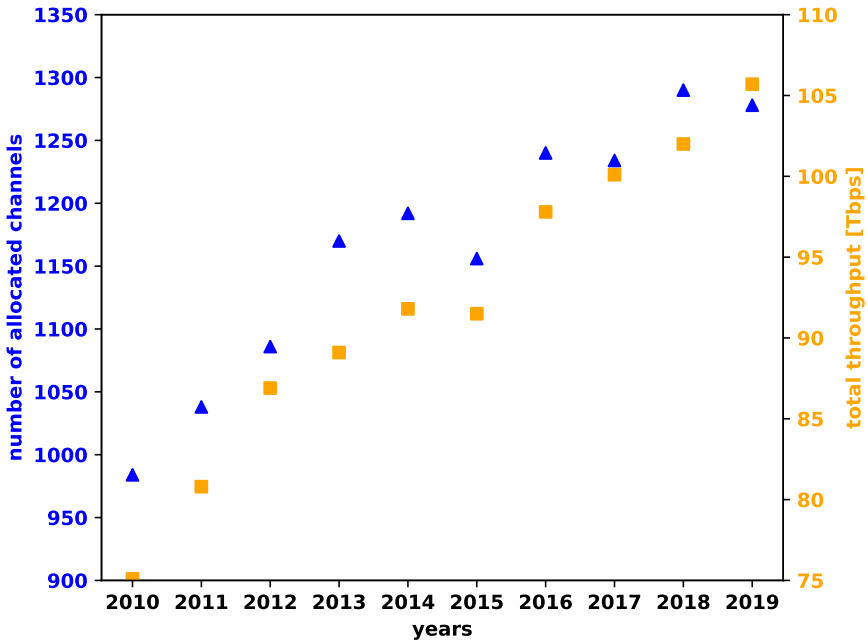

Fig. 6: Relationship between number of occupied channels (black triangles) and total capacity (grey squares) for empirical data in 2010 – 2019.

ICCS Camera Ready Version 2021
To cite this paper please use the final published version:
DOI: 10.1007/978-3-030-77970-2_28

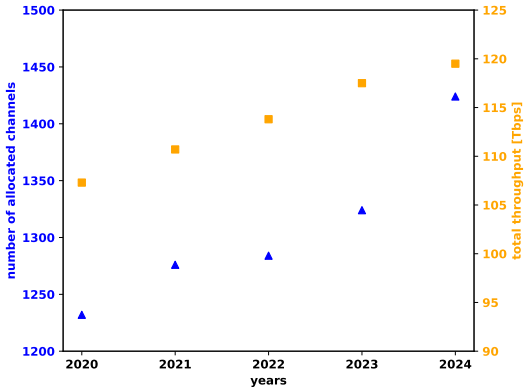

(a) forecast (level Min)

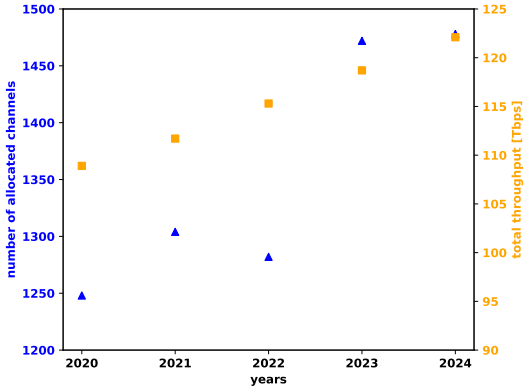

(b) forecast (level 0)

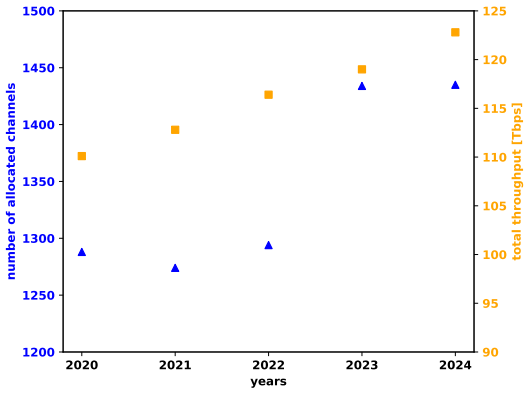

(c) forecast (level Max)

Fig. 7: Relationship between number of occupied channels (black triangles) and total capacity (grey squares) for forecast data.

ICCS Camera Ready Version 2021
To cite this paper please use the final published version:
DOI: 10.1007/978-3-030-77970-2_28

Figures 6 and 7 show optical bandwidth utilisation (number of occupied optical channels) and total network capacity (throughput) for empirical and forecast data (in 2020 – 2024). Based on the presented results one can observe that:

- the increase in number of optical channels roughly corresponds to the increase in throughput for the empirical data,
- growth of total throughput for forecasts is nearly linear, while there is a large deviation from linearity for the number of optical channels.

4 Conclusion

The paper presents the analysis of fiber bandwidth utilization in DWDM optical network using statistical methods for the estimation of the demands matrix. The presented study provides methods for forecasting the matrix of traffic demands for the next years and for identification of both the bottlenecks in the network and network edges that are not used. Such an analysis is very useful to the telecommunication network operators, as it allows for optimal use of the allocated resources and aids the process of network expansion planning. This is because the results obtained allow assessing the need for additional investment into the DWDM network infrastructure. Hence, the developed model predicts the network edges that are most likely to be subjected to traffic congestion. This allows the network operator to plan in advance the network expansion and allocate appropriate means for the necessary capital expenditure.

To the best of the authors' knowledge, there are no publications in available literature on the problem considered in this contribution. Thus, this paper in a way initiates this topic and potentially can become a benchmark for future research.

Further research will be focused on improving the stochastic forecasting model to include the access and backbone network interfaces. In addition, modeling different network expansion scenarios taking into account existing network topologies and additional edge extensions. The cost function will include part of capital expenditures and operating expenditures. Additionally, we plan to use nature-inspired algorithms as additional heuristic methods to solve the problem.

References

1. ctc technology & energy: Dark fiber lease considerations. Tech. rep. (2012), `www.ctcnet.us/DarkFiberLease.pdf`, accessed on 2019-08-29
2. Becker, P.M., Olsson, A.A., Simpson, J.R.: Erbium-Doped Fiber Amplifiers: Fundamentals and Technology. Elsevier (1999)
3. Cai, A., Shen, G., Peng, L., Zukerman, M.: Novel node-arc model and multiiteration heuristics for static routing and spectrum assignment in elastic optical networks. J. Lightwave Technol. **31**(21), 3402–3413 (Nov 2013), `http://jlt.osa.org/abstract.cfm?URI=jlt-31-21-3402`

ICCS Camera Ready Version 2021
To cite this paper please use the final published version:
DOI: 10.1007/978-3-030-77970-2_28

4. Dallaglio, M., Giorgetti, A., Sambo, N., Velasco, L., Castoldi, P.: Routing, spectrum, and transponder assignment in elastic optical networks. Jour. of Lightwave Technol. **33**(22), 4648–4658 (Nov 2015). https://doi.org/10.1109/JLT.2015.2477898
5. Desurvire, E., Bayart, D., Desthieux, B., Bigo, S.: Erbium-Doped Fiber Amplifiers: Device and System Developments. Wiley (2002)
6. Klinkowski, M., Walkowiak, K.: Routing and spectrum assignment in spectrum sliced elastic optical path network. IEEE Communications Letters **15**(8), 884–886 (August 2011). https://doi.org/10.1109/LCOMM.2011.060811.110281
7. Klinkowski, M., Żotkiewicz, M., Walkowiak, K., Pióro, M., Ruiz, M., Velasco, L.: Solving large instances of the RSA problem in flexgrid elastic optical networks. IEEE/OSA Journal of Optical Communications and Networking **8**(5), 320–330 (May 2016). https://doi.org/10.1364/JOCN.8.000320
8. Kozdrowski, S., Żotkiewicz, M., Sujecki, S.: Optimization of optical networks based on CDC-ROADM technology. Applied. Sciences. **9**(3) (2019). https://doi.org/10.3390/app9030399, `http://www.mdpi.com/2076-3417/9/3/399`
9. Kozdrowski, S., Żotkiewicz, M., Sujecki, S.: Ultra-wideband wdm optical network optimization. Photonics **7**(1) (2020). https://doi.org/10.3390/photonics7010016, `https://doi.org/10.3390/photonics7010016`
10. Orlowski, S., Wessäly, R., Pióro, M., Tomaszewski, A.: Sndlib 1.0-survivable network design library. Networks **55**(3), 276–286 (2010). https://doi.org/10.1002/net.20371, `https://onlinelibrary.wiley.com/doi/abs/10.1002/net.20371`
11. Poggiolini, P., Bosco, G., Carena, A., Curri, V., Jiang, Y., Forghieri, F.: The GN-model of fiber non-linear propagation and its applications. Journal of Lightwave Technology **32**(4), 694–721 (Feb 2014). https://doi.org/10.1109/JLT.2013.2295208
12. Shariati, B., Mastropaolo, A., Diamantopoulos, N., Rivas-Moscoso, J.M., Klonidis, D., Tomkos, I.: Physical-layer-aware performance evaluation of SDM networks based on SMF bundles, MCFs, and FMFs. IEEE/OSA J. Opt. Com.&N. **10**(9), 712–722 (Sep 2018). https://doi.org/10.1364/JOCN.10.000712
13. Sliwka, P.: Proposed methods for modeling the mortgage and reverse mortgage installment. In: Recent Trends In The Real Estate Market And Its Analysis. Oficyna Wydawnicza SGH,Warszawa (2018) pp. 189–206 (2018)
14. Sliwka, P.: Application of the model with a non-gaussian linear scalar filters to determine life expectancy, taking into account the cause of death. In: Rodrigues J. et al. (eds) Computational Science – ICCS 2019.LNCS, Springer, Cham (2019) **11538**, 435–449 (2019). https://doi.org/10.1007/978-3-030-22744-9_34
15. Sliwka, P., Socha, L.: A proposition of generalized stochastic milevsky-promislov mortality models. SCAND ACTUAR J pp. 706–726 (2018)
16. Sliwka, P., Swistowska, A.: Economic forecasting methods with the R package. Wydawnictwo Naukowe UKSW (2019)
17. de Sousa, A., Monteiro, P., Lopes, C.B.: Lightpath admission control and rerouting in dynamic flex-grid optical transport networks. Networks **69**(1), 151–163 (2017). https://doi.org/10.1002/net.21715, `https://onlinelibrary.wiley.com/doi/abs/10.1002/net.21715`
18. Żotkiewicz, M., Ruiz, M., Klinkowski, M., Pióro, M., Velasco, L.: Reoptimization of dynamic flexgrid optical networks after link failure repairs. IEEE/OSA Journal of Optical Communications and Networking **7**(1), 49–61 (Jan 2015). https://doi.org/10.1364/JOCN.7.000049

ICCS Camera Ready Version 2021
To cite this paper please use the final published version:
DOI: 10.1007/978-3-030-77970-2_28